Future Generation Computer Systems 87 (2018) 127–135

Contents lists available at ScienceDirect

Future Generation Computer Systems

journal homepage: www.elsevier.com/locate/fgcs

Age-related Macular Degeneration detection using deep convolutional neural network

Jen Hong Tan [a], Sulatha V. Bhandary [b], Sobha Sivaprasad [c], Yuki Hagiwara [a,*], Akanksha Bagchi [c], U. Raghavendra [d], A. Krishna Rao [b], Biju Raju [e], Nitin Shridhara Shetty [f], Arkadiusz Gertych [g], Kuang Chua Chua [a], U. Rajendra Acharya [a,h,i]

[a] Department of Electronics and Computer Engineering, Ngee Ann Polytechnic, Singapore
[b] Department of Ophthalmology, Kasturba Medical College, Manipal, India
[c] NIHR Moorfields Biomedical Research Centre, London, UK
[d] Department of Instrumentation and Control Engineering, Manipal Institute of Technology, Manipal Academy of Higher Education, India
[e] Dr. NSD Raju's Eye Hospital and Research Centre, Kochi, Kerala, India
[f] Vitreoretina Consultant, Department of Ophthalmology, Manipal Hospital, Bangalore, India
[g] Department of Surgery, Department of Pathology and Laboratory Medicine, Cedars-Sinai Medical Center, Los Angeles, CA, USA
[h] Department of Biomedical Engineering, School of Science and Technology, Singapore School of Social Sciences, Singapore
[i] Department of Biomedical Engineering, Faculty of Engineering, University of Malaya, Malaysia

HIGHLIGHTS

- Automated detection of age-related macular degeneration(AMD) with fundus images.
- A 14-layer convolutional neural network is employed.
- Trained and tested on 402 normal and 708 AMD images.
- Achieved an average accuracy of 95.45% with ten-fold cross validation.
- Achieved an average accuracy of 91.17% with blindfold.

GRAPHICAL ABSTRACT

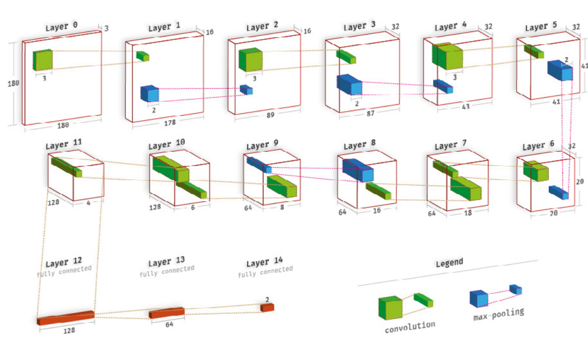

ARTICLE INFO

Article history:
Received 30 August 2017
Received in revised form 19 April 2018
Accepted 1 May 2018
Available online 29 May 2018

Keywords:
Age-related Macular Degeneration
Aging
Computer-aided diagnosis system
Convolutional neural network
Deep learning
Fundus images

ABSTRACT

Age-related Macular Degeneration (AMD) is an eye condition that affects the elderly. Further, the prevalence of AMD is rising because of the aging population in the society. Therefore, early detection is necessary to prevent vision impairment in the elderly. However, organizing a comprehensive eye screening to detect AMD in the elderly is laborious and challenging. To address this need, we have developed a fourteen-layer deep Convolutional Neural Network (CNN) model to automatically and accurately diagnose AMD at an early stage. The performance of the model was evaluated using the blindfold and ten-fold cross-validation strategies, for which the accuracy of 91.17% and 95.45% were respectively achieved. This new model can be utilized in a rapid eye screening for early detection of AMD in the elderly. It is cost-effective and highly portable, hence, it can be utilized anywhere.

1. Introduction

The world is currently facing an aging population with approximately 962 million people aged 60 years or above [1]. This number

* Corresponding author.
E-mail address: yukihagiwara92@gmail.com (Y. Hagiwara).

https://doi.org/10.1016/j.future.2018.05.001

is expected to double to 2 billion people by 2050 [1]. With such a rapid growth in aging population, it is inevitable that the Global Burden of Disease (GBD) among the elderly increases too [2]. The rise of GBD is associated with higher medical costs and lower quality of life affecting not only the aged people but also their caregivers and the health economy [3]. Co-morbidities in the aging population often cause further delay in early diagnosis of treatable conditions. Therefore, there is an unmet need to develop simple, cheap and portable diagnostic and analytical tools to allow early diagnosis and prompt referral for treatment [4].

Age-related Macular Degeneration (AMD) is one of the conditions commonly faced by the elderly. It is the prime cause of vision loss in elderly (>50 years old) [5–8]. AMD is a chronic eye condition that affects the central vision of the eye [9]. It is due to the degeneration of the macula, the central part of the retina that subserves clear and sharp vision [9].

Typically, AMD can be characterized by four stages (no, early, intermediate, and advanced) [10]. No AMD is graded when there is no or a few small drusen (macular yellow deposits) present. Early AMD is graded if there is small to medium-sized drusen [10]. Intermediate AMD is characterized by at least one large-sized drusen or a handful of medium-sized drusen with or without pigmentary changes. Advanced AMD may be dry or wet types. Dry AMD is graded as Geographic Atrophy (GA) when there is loss or atrophy of the retinal pigment epithelium at the macula. This atrophic area progresses slowly to the center of the macula. Center-involving GA leads to an irreversible loss of vision [10]. The wet AMD, on the contrary, is more sudden in onset and progresses rapidly. Wet AMD occurs as a result of an abnormal growth of blood vessels beneath the retina, that may leak or bleed causing a rapid decline in vision [10].

There are no symptoms present at an early stage of AMD. Some symptoms such as blurred or distorted vision may appear in intermediate while visual acuity invariably deteriorates in advanced AMD [9]. Timely detection and treatment impede further deterioration in vision in wet AMD. Hence, it is of utmost importance for an early diagnosis of wet AMD to prevent progressive visual impairment in the elderly. AMD can be diagnosed using fundus photography. Fundus photography is the preferred tool for classifying the severity of AMD.

However, the visual interpretation of fundus images can be subjective and is prone to interobserver variabilities. Thus, a Computer-Aided Diagnosis (CAD) system is proposed to aid in the objective and reliable assessment of fundus images. A lot of studies have been done on the automated identification of AMD fundus images. However, no attempt of implementing deep learning solutions has so far been proposed to support AMD detection.

Therefore, a fourteen-layer deep Convolutional Neural Network (CNN) is proposed to automatically classify the fundus images into normal or AMD classes in this work. In contrast to other studies, no handcrafted features are required. Instead, fundus images are fed into the proposed model and a diagnosis is given almost instantaneously.

CNN is a subclass of a multilayer Neural Networks (NN) and it is one of the architectures in deep learning. It is a computational model based on the biological neural networks in the human brain [11]. CNN has been gaining recognition in analyzing medical image data [11,12]. Some applications of CNNs to analyze retinal images have already been published. For instance, van Grinsven et al. [13] applied CNN to identify hemorrhages in fundus images. They applied a nine-layer CNN model in their work. Also, a seven-layer deep CNN was employed to concurrently locate and segment fovea, optic disk, and vasculature from fundus images [14]. The high accuracy performance of the proposed CNN model highlights the potential capabilities of CNN in CAD systems. CNNs can also be applied in other CAD applications including the detection of arrhythmia [15], coronary artery disease [16], and myocardial infarction [17]. Furthermore, CNN models have revealed outstanding recognition ability in visual recognition assignments [12,18].

The performance of the model was evaluated using the blindfold and ten-fold cross-validation strategies, for which the accuracy of 91.17% and 95.45% were respectively achieved. This new model can be utilized in a rapid eye screening for early detection of AMD in the elderly. It is cost-effective and highly portable; hence, it can be utilized anywhere. The design the deep learning model for the dry and wet AMD images is the novelty of this paper.

2. Data

The data used in this work were acquired from the Ophthalmology Department of Kasturba Medical College (KMC), Manipal, India. We have obtained ethics approval to collect the fundus images from Kasturba Medical Hospital, Manipal to conduct this study. We evaluated 402 eyes with normal fundus, 583 retinal images with early, intermediate AMD, or GA and 125 retinal images with evidence of wet AMD.

The images collected were acquired using Zeiss FF450 plus mydriatic fundus camera with the image resolution of 2588 × 1958 pixels. Examples of normal and AMD (dry and wet) fundus image can be seen in Fig. 1.

3. Methods

The architecture of the proposed model is listed in Table 1. The proposed model has seven convolution layers, four max-pooling layers, and three fully-connected layers. Fig. 2 shows a graphical illustration of the proposed CNN model.

The CNN architecture is made up of convolution, pooling, and fully-connected layer [11,19]. The main purpose of the convolution operation is to pick up distinct features from the input fundus image. The convolution is performed with convolution filters (kernels) to generate feature maps [11,20]. The pooling operation reduces the output dimensionality and ensures a fixed output size. The max-pooling operation is performed in this study. This operation takes the highest value from each kernel, reducing the size of the feature maps. The stride (number of units the filter slides) for convolution and max-pooling is set at 1 and 2 respectively in this work. The fully-connected layer uses a softmax activation function for the output layer. The main purpose is to predict the input fundus image into normal or AMD classes.

Each image was rescaled to 180 × 180 dimension. The input layer which consists of size 180 × 180 × 3 where each dimension represents height, width and channel respectively is convolved with 16 3 × 3 × 3 kernels to form layer 1. Then a max-pooling of 2 × 2 is performed. After which, a convolution is performed again in layer 2 with 32 3 × 3 × 16 kernels, followed by a 2 × 2 max-pooling operation to form layer 4. Once again, a convolution is applied on 32 feature maps in layer 4 to form layer 5. Then, a max-pooling is applied in layer 6. Then, convolution is performed again in layers 6, 7, and 8 before a max-pooling of size 2 × 2 is applied. Convolution is again applied to 64 feature maps in layer 9 and convolved again in layer 10 to produce 4 × 4 × 128 number of neurons (layer 11). The neurons in layer 11 are fully-connected to 128 neurons in layer 12. Also, layer 12 is fully-connected to 64 neurons in layer 13 and fully-connected to layer 14 (the output layer) with an output of 2 neurons to represent normal and AMD classes.

(a) Normal. (b) Dry AMD. (c) Wet AMD.

Fig. 1. Examples of healthy (a), dry AMD (b), and (c) wet AMD fundus images.

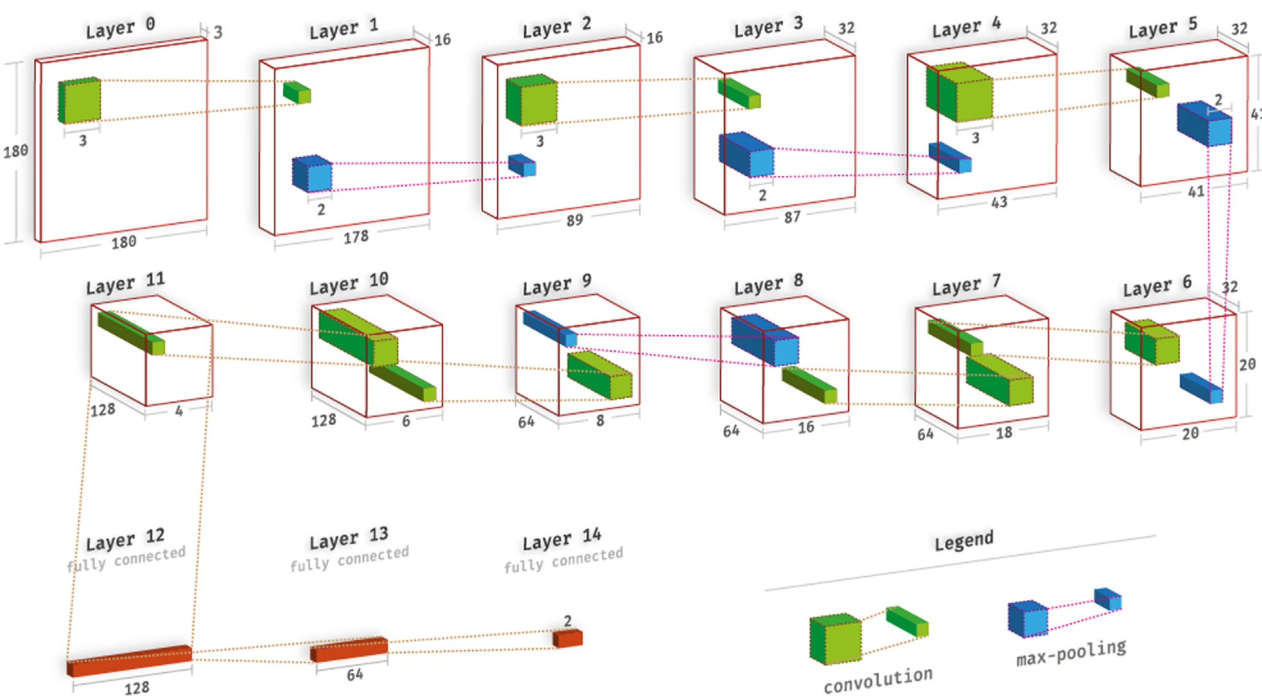

Fig. 2. An illustration of the proposed CNN architecture for this work.

Table 1
The details of proposed CNN architecture for this work.

Layers	Type	Number of feature maps	Number of neurons in the layer	The size of the kernel involves to form each feature map	Stride	Number of trainable parameters
0	Input	3	180 × 180 × 3	–	–	0
1	Convolution	16	178 × 178 × 16	3 × 3 × 3	1	448
2	Max-pooling	16	89 × 89 × 16	2 × 2	2	0
3	Convolution	32	87 × 87 × 32	3 × 3 × 16	1	4 640
4	Max-pooling	32	43 × 43 × 32	2 × 2	2	0
5	Convolution	32	41 × 41 × 32	3 × 3 × 32	1	9 248
6	Max-pooling	32	20 × 20 × 32	2 × 2	2	0
7	Convolution	64	18 × 18 × 64	3 × 3 × 32	1	18 496
8	Convolution	64	16 × 16 × 64	3 × 3 × 64	1	36 928
9	Max-pooling	64	8 × 8 × 64	2 × 2	2	0
10	Convolution	128	6 × 6 × 128	3 × 3 × 64	1	73 856
11	Convolution	128	4 × 4 × 128	3 × 3 × 128	1	147 584
12	Fully-connected	–	128	–	–	262 272
13	Fully-connected	–	64	–	–	8 256
14	Fully-connected	–	2	–	–	130
					Total	561 858

Table 2
Data used in this study.

Blindfold		Ten-fold	
Normal	402	Normal	400
AMD	708	AMD	700

4. Training and testing

The CNN model was trained using backpropagation [21] with a batch size of 50. Moreover, 'Adam' algorithm [22] was employed to optimize the learning parameters of the CNN model. The following default settings were used to train the model: $\alpha = 0.001$, $\beta_1 = 0.9$, $\beta_2 = 0.999$, and $\epsilon = 10^{-8}$, where α represents the learning rate, β_1, $\beta_2$denote the exponential decay rates, and ϵ is numerical value — epsilon.

The 'Adam' algorithm is an optimizer whereby it estimates the adaptive learning rate based on moments. Therefore, little tuning of the parameters is required. Besides that, Adam is widely adopted in the deep learning model training by other groups [23].

In this work, blindfold and ten-fold cross-validation strategies were used to validate the performance of the proposed CNN model. A total of 1110 and 1100 fundus images were used in the blindfold and augmented ten-fold strategies respectively (refer to Table 2). For the ten-fold cross-validation strategy, the model was trained in ten iterations. First, the training data (400 normal and 700 fundus images) was divided into ten segments. Then, nine out of ten segments were used for training, and the tenth segment is used for validation. Further, the images were augmented four times for training:

1. The original fundus images.
2. The original fundus images flipped to the left.
3. The original fundus images flipped downwards.
4. The original fundus images flipped to the left then downwards.

The fundus images were augmented by translating the images in different directions (left and down) and at the same time, producing more images to train the model. Data augmentation also prevented overfitting of data.

On the other contrary, in the blindfold approach, the data was randomly split into two sets for training and testing the proposed model respectively.

5. Results

The proposed CNN model is trained on a workstation with two Intel Xeon 2.20 GHz (E5-2650 v4) processor and a 512 GB Random Access Memory (RAM) without any Graphics Processing Unit (GPU) support. It took typically 106 to 110 s (blindfold) and approximately 176 to 190 s (ten-fold) to complete an epoch. 60 epochs in total were run in this study. The proposed CNN model is developed and trained using Keras with Theano backend [24].

The parameters used to compute the diagnostic performance of the proposed model are accuracy, sensitivity, and specificity [25]. The accuracy determines the capability of the model to differentiate the normal and AMD fundus images, sensitivity computes the ability of the model to correctly identify AMD fundus images and specificity calculates the competency of the model to accurately classify the normal fundus images.

Tables 3 and 4 show the overall performance results using the two validation [26,27] (blindfold and ten-fold) approaches respectively. Based on Table 5, none of the works implemented the blindfold strategy. Hence, the blindfold strategy is performed in this study. A relatively good performance of 91.17% accuracy, 92.66% sensitivity, and 88.56% specificity is obtained using the blindfold strategy (see Table 3). This shows that the proposed system is robust and is capable of identifying an unknown fundus image.

Table 3
Results obtained using blindfold strategy.

TP	FN	TN	FP	Accuracy	Sensitivity	Specificity
328	26	178	23	0.9117	0.9266	0.8856

TP = True Positive, FN = False Negative, TN = True Negative, FP = False Positive.

Table 4
Results obtained using ten-fold cross-validation strategy.

Fold	TP	FN	TN	FP		Accuracy	Sensitivity	Specificity
1	67	3	34	6		0.9182	0.9571	0.8500
2	70	0	37	3		0.9727	1.0000	0.9250
3	67	3	39	1		0.9636	0.9571	0.9750
4	69	1	39	1		0.9818	0.9857	0.9750
5	68	2	38	2		0.9636	0.9714	0.9500
6	67	3	39	1		0.9636	0.9571	0.9750
7	63	7	38	2		0.9182	0.9000	0.9500
8	67	3	38	2		0.9545	0.9571	0.9500
9	68	2	37	3		0.9545	0.9714	0.9250
10	69	1	36	4		0.9545	0.9857	0.9000
					Average	0.9545	0.9643	0.9375

TP = True Positive, FN = False Negative, TN = True Negative, FP = False Positive.

In Table 4, it is noted that desirable results are obtained in each fold. A total of ten folds is validated in each iteration and the average of the overall performance is obtained with an accuracy of 95.45% with a sensitivity of 96.43% and specificity of 93.75%.

6. Discussion

It is observed that most of the past works achieved high performance in classifying AMD with a small number of data set. This is because, in conventional machine learning technique, there is a pipeline to follow: (i) preprocessing, (ii) feature extraction, (iii) feature selection, and (iv) classification. Consequently, a set of highly significant features extracted will be fed into the classifier for classification. However, an engineered set of features is data dependent. Thus, using a small number of images with little variations tend to yield better performances. Also, one can note, that in contrast to previous studies, this work utilized the highest number of fundus images (402 normal and 708 AMD). This dataset came from various databases, that were combined to provide a more diverse range of fundus images for training and testing of the proposed CNN model.

The proposed CNN model has achieved high performance with blindfold and ten-fold cross-validation strategies respectively. This indicates the robustness of the model. In our proposed model, at the convolution layer the features extracted are distinct for the normal and AMD classes. Also, we have used 402 normal, 583 dry AMD, and 125 wet AMD images. High classification performance in blindfold and ten-fold cross-validation indicates that, we have obtained high performance in each fold indicating the superiority of the developed system. But, however, with more images we will be able to improve the performance further.

In the past studies Köse et al. [28,29] employed segmentation techniques to automatically identify the two classes of fundus images. Their proposed techniques achieved an accuracy of at least 90.00%. However, in their work, there are various preprocessing steps to segment and classify fundus images. Recently, Tan et al. [14] introduced a seven-layer CNN to simultaneously locate and segment fovea, optic disk, and retinal vasculature with an average accuracy of 92.68%. This technique demonstrated the competency of CNN in generalizing features.

Table 5
A summary of selected works on the automated identification of normal and AMD classes.

Author	Year	Number of images (Database)	Techniques	Performance
Köse et al. [28]	2008	N: 30 AMD: 30 (KTU)	Segmentation	Acc: <90.00%
Köse et al. [29]	2010	N: 40 AMD: 40 (KTU)	Segmentation	Acc: 98.75%
Agurto et al. [32]	2011	N: 64 AMD: 247 (RIST) N: 116 AMD: 271 (UTHSCSA)	AM-FM PLS classifier	Auc: 0.81 (RIST) Auc: 0.89 (UTHSCSA)
Zheng et al. [33]	2012	N: 98 AMD: 160 (ARIA and STARE)	Weighted frequent sub-graph mining	Ten-fold: Acc: 99.60% Sen: 99.40% Spec: 100.00%
Hijazi et al. [34]	2012	N: 60 AMD: 101 (ARIA)	Hierarchical decomposition (1,262 features)	Ten-fold: Acc: 100.00% Sen: 100.00% Spec: 100.00%
Mookiah et al. [36]	2014	N: 101 AMD: 60 (ARIA) N: 270 AMD: 270 (KMC) N: 36 AMD: 47 (STARE)	Entropies, HOS, fractal dimension, RT, Gabor wavelet SVM-linear classifier	Ten-fold: Acc: 95.07% Sen: 96.09% Spec: 93.33% (ARIA) Acc: 90.19% Sen: 88.89% Spec: 91.48% (KMC) Acc: 95.00% Sen: 96.00% Spec: 93.33% (STARE)
Mookiah et al. [37]	2014	N: 270 AMD: 270 (KMC)	Energy, entropies, DWT, first-order statistics SVM-linear classifier	Ten-fold: Acc: 93.70% Sen: 91.11% Spec: 96.30%
Hijazi et al. [35]	2015	N: 98 AMD: 165 (AMD and STARE)	Tree-based approach	Ten-fold: Acc: 99.90% Sen: 100.00% Spec: 99.00%
Mookiah et al. [38]	2015	N: 101 AMD: 60 (ARIA) N: 270 AMD: 270 (KMC) N: 36 AMD: 47 (STARE)	EMD, entropies, HOS, RT SVM classifier	Ten-fold: Acc: 85.09% Sen: 86.14% Spec: 83.33% (ARIA) Acc: 91.67% Sen: 90.74% Spec: 92.59% (KMC) Acc: 100.00% Sen: 100.00% Spec: 100.00% (STARE) Acc: 84.06% Sen: 82.30% Spec: 86.07% (combined)

(*continued on next page*)

Moreover, Acharya et al. [30] proposed an AMD diagnosis tool to diagnose normal, dry AMD, and wet AMD. This was the first study on the classification of a three-class AMD fundus images. Despite the novelty of a three-class AMD diagnosis problem, it is not implemented in this study because AMD was not classified according to the most recent classification [31].

Table 5 (*continued*)

Author	Year	Number of images (Database)	Techniques	Performance
Mookiah et al. [39]	2015	N: 101 AMD: 60 (ARIA) N: 270 AMD: 270 (KMC) N: 36 AMD: 47 (STARE)	LCP SVM-MV classifier	Ten-fold: Acc: 90.68% Sen: 90.10% Spec: 91.67% (ARIA) Acc: 92.96% Sen: 90.00% Spec: 95.93% (KMC) Acc: 97.59% Sen: 97.87% Spec: 97.22% (STARE)
Acharya et al. [40]	2016	N: 101 AMD: 60 (ARIA) N: 404 AMD: 381 (KMC) N: 36 AMD: 47 (STARE)	DWT, RT AMD index SVM-RBF classifier DT classifier	Ten-fold: Acc: 96.89% Sen: 100.00% Spec: 91.67% (ARIA) Acc: 99.49% Sen: 99.21% Spec: 99.75% (KMC) Acc: 100.00% Sen: 100.00% Spec: 100.00% (STARE)
Acharya et al. [30]	2017	N: 404 Dry AMD: 517 Wet AMD: 24 (KMC)	PHOG, nonlinear features SVM classifier	Ten-fold: Acc: 83.30% Sen: 82.60% Spec: 84.80%
In this work	**2017**	**N: 402** **AMD: 708** **(KMC)**	**14-layer deep CNN**	**Blindfold:** **Acc: 91.17%** **Sen: 92.66%** **Spec: 88.56%** **Ten-fold:** **Acc: 95.45%** **Sen: 96.43%** **Spec: 93.75%**

KTU: Karadeniz Technical University; RIST: Retina Institute of South Texas; UTHSCSA: University of Texas Health Science Center in San Antonio; ARIA: Automated Retinal Image Analysis; STARE: STructured Analysis of the Retina; KMC: Kasturba Medical College.
PHOG: Pyramid Histogram of Oriented Gradients
N: Normal
Acc: Accuracy; Auc: Area under curve; Sen: Sensitivity, Spec: Specificity.

In addition, based on Table 5, it can be noted that various researchers have conducted studies on the automated identification of normal and AMD using fundus images. Moreover, relatively high diagnostic performances were achieved using their proposed methodologies. Agurto et al. [32] employed the Amplitude-Modulation and Frequency-Modulation (AM–FM) method to distinguish the two classes of fundus images obtained from two different databases with an Area Under Curve (AUC) value of more than 0.8 using Partial Least Square (PLS) classifier. Zheng et al. [33] have also shown the effectiveness of their algorithm with an accuracy of 99.60%. They carried out an image mining approach to extract significant features for classification in this work. They reported 99.40% and 100% sensitivity and specificity respectively.

Hijazi et al. [34] attained 100% accuracy in the differentiation of normal and AMD fundus images using hierarchical decomposition using 60 normal and 101 AMD fundus images from a public database. In another work by Hijazi et al. [35], they employed a tree-based technique to identify the AMD fundus images from normal fundus images with a diagnostic performance of 99.90%. Mookiah et al. [36–39] investigated different methodologies to design a robust CAD AMD system. They have extracted entropies [36–38], Empirical Mode Decomposition (EMD) [38], Higher-Order Spectra (HOS) [36,38], and Local Configuration Pattern (LCP) [39] features from the fundus images. They have employed the Support Vector Machine (SVM) classifier in their studies.

Acharya et al. [40] demonstrated 100% diagnostic accuracy in the identification of normal and AMD fundus images using a public database. They have used Radon Transform (RT) technique to convert the two-dimensional fundus image into one-dimensional signals before applying Discrete Wavelet Transform (DWT) to extract the concealed signatures from the decomposed signals. Furthermore, they developed an AMD index that could numerically distinguish the two classes with an integer.

Regardless of the high diagnostic performance reported in Table 5, the advantages of our proposed model outweigh them. The advantages are first, the proposed model is fully automatic. There is no hand-crafted feature extraction or selection. Also, no classifier is required for this proposed model. The conventional machine learning techniques listed in Table 5 require manual features extraction, features selection, and classification. They involve meticulous engineering to design a feature extraction that could extract highly distinctive features to be inserted into a classifier for classification [41]. Secondly, the proposed model can be installed in cloud system. The test image can be sent to the cloud for classification through web browser. The result of the classification will be sent back from the web server. The Optical Coherence Tomography (OCT) is a diagnostic tool that is superior and commonly used to diagnose the different eye conditions [42]. However, this machine is heavy, immobile and expensive. Therefore, the proposed model has additional benefits as compared to the existing OCT machine. Hence, it is suitable to be employed in polyclinics to aid ophthalmologists in their diagnosis. Moreover, the proposed model can be easily installed as a CAD eye screening tool to assist in fundus screening sessions.

On the other hand, the proposed model requires big data with ground truths labeled for training to achieve maximum performance. But, the overall diagnostic performance of the proposed CNN model will improve with a larger number of data. Furthermore, the CNN model is highly complex and associates with problems of convergence and overfitting. Nevertheless, the parameters in the proposed model are constantly adjusted to achieve maximum performance. In addition, the training of CNN model is slow and intensive. Nonetheless, once the CNN model is trained, the testing of the fundus images is fast and accurate.

7. Conclusion

This paper proposes a novel technique to accurately detect AMD using a custom designed CNN. High classifier accuracies of 91.17% and 95.45% are obtained with the blindfold and ten-fold cross-validation strategies respectively. Furthermore, no engineered features are required for the diagnosis using fundus images. Also, the proposed model is fully autonomous therefore, it can be effortlessly applied to clinics. This proposed CAD system for AMD can serve as a second opinion tool to assist ophthalmologists in their diagnosis. It can also be installed in third world countries or in rural areas where ophthalmology care is limited.

Acknowledgment

The authors would like to express your since thanks to all the staffs in the Department of Ophthalmology in KMC, Manipal, for their assistance in obtaining the fundus images from the patients.

References

[1] Department of Economic and Social Affairs, World Population Prospects The 2017 Revision Key Findings and Advance Tables, United Nations, New York, 2017.
[2] M.J. Prince, et al., The burden of disease in older people and implications for health policy and practice, Lancet 385 (9967) (2015) 549–562.
[3] J.L. Prenner, L.S. Halperin, C. Rycroft, S. Hogue, Z. Williams Liu, R. Seibert, Disease burden in the treatment of age-related macular degeneration: findings from a time-and-motion study, Am. J. Ophthalmol. 160 (4) (2015) 725–731e1.
[4] World Health Organization, World report on ageing and health, 2017.
[5] National Eye Institute, Facts about age-related macular degeneration, 2015 (Online). Available: https://nei.nih.gov/health/maculardegen/armd_facts. (Accessed 28 July 2017).
[6] J.E.W. Koh, E.Y.K. Ng, S.V. Bhandary, Y. Hagiwara, A. Laude, U.R. Acharya, Automated retinal health diagnosis using pyramid histogram of visual words and fisher vector techniques, Comput. Biol. Med. 92 (2018).
[7] J.E.W. Koh, et al., Diagnosis of retinal health in digital fundus images using continuous wavelet transform (cwt) and entropies, Comput. Biol. Med. 84 (2017).
[8] J.E.W. Koh, E.Y.K. Ng, S.V. Bhandary, A. Laude, U.R. Acharya, Automated detection of retinal health using phog and surf features extracted from fundus images, Appl. Intell. (2017) 1–15.
[9] L.S. Lim, P. Mitchell, J.M. Seddon, F.G. Holz, T.Y. Wong, Age-related macular degeneration, Lancet 379 (9827) (2012) 1728–1738.
[10] S.J. Ryan, A.P. Schachat, C.P. Wilkinson, D.R. Hinton, S.R. Sadda, P. Wiedemann, Retina, 5th ed. Expert Consult Premium Edition: Enhanced Online Features and Print, 3-Volume Set, 2012.
[11] J.-G. Lee, et al., Deep learning in medical imaging: general overview, Korean J. Radiol. 18 (4) (2017) 570.
[12] H. Greenspan, B. van Ginneken, R.M. Summers, Guest editorial deep learning in medical imaging: overview and future promise of an exciting new technique, IEEE Trans. Med. Imaging 35 (5) (2016) 1153–1159.
[13] M.J.J.P. Van Grinsven, B. Van Ginneken, C.B. Hoyng, T. Theelen, C.I. Sanchez, Fast convolutional neural network training using selective data sampling: application to hemorrhage detection in color fundus images, IEEE Trans. Med. Imaging 35 (5) (2016) 1273–1284.
[14] J.H. Tan, U.R. Acharya, S.V. Bhandary, K.C. Chua, S. Sivaprasad, Segmentation of optic disc, fovea and retinal vasculature using a single convolutional neural network, J. Comput. Sci. 20 (2017) 70–79.
[15] U.R. Acharya, H. Fujita, S.L. Oh, Y. Hagiwara, J.H. Tan, M. Adam, Automated detection of arrhythmias using different intervals of tachycardia ecg segments with convolutional neural network, Inf. Sci. (Ny). 405 (2017).
[16] U.R. Acharya, H. Fujita, S.L. Oh, M. Adam, J.H. Tan, K.C. Chua, Automated detection of coronary artery disease using different durations of ecg segments with convolutional neural network, Knowledge-Based Syst. 946 (2017) 1–10.
[17] U.R. Acharya, H. Fujita, S.L. Oh, Y. Hagiwara, J.H. Tan, M. Adam, Application of deep convolutional neural network for automated detection of myocardial infarction using ecg signals, Inf. Sci. (Ny). 416 (2017) 190–198.
[18] K. He, X. Zhang, S. Ren, J. Sun, Delving deep into rectifiers: Surpassing human-level performance on imagenet classification, in: Proceedings of the IEEE International Conference on Computer Vision, vol. 11–18–Dec, 2016, pp. 1026–1034.
[19] A. Krizhevsky, I. Sutskever, G.E. Hinton, Imagenet classification with deep convolutional neural networks, Adv. Neural Inf. Process. Syst. (2012) 1–9.
[20] B. Zhao, H. Lu, S. Chen, J. Liu, D. Wu, Convolutional neural networks for time series classification, J. Syst. Eng. Electron. 28 (1) (2017) 162–169.
[21] J. Bouvrie, Notes on convolutional neural networks, In Pract. 12 (2006) 47–60.
[22] D.P. Kingma, J. Ba, Adam: A Method for Stochastic Optimization, Iclr, 2015, pp. 1–15.
[23] S. Ruder, An overview of gradient descent optimization algorithms, Web Page, 2016, pp. 1–12.
[24] Theano Development Team, Theano: A Python framework for fast computation of mathematical expressions, 2016. ArXiv e-prints, p. 19.
[25] K.J. Van Stralen, V.S. Stel, J.B. Reitsma, F.W. Dekker, C. Zoccali, K.J. Jager, Diagnostic methods I: sensitivity, specificity, and other measures of accuracy, Kidney Internat. 75 (12) (2009) 1257–1263.
[26] L.P. Devroye, T.J. Wagner, Distribution-free performance bounds for potential function rules, IEEE Trans. Inform. Theory 25 (5) (1979) 601–604.
[27] R.O. Duda, P.E. Hart, D.G. Stork, Pattern Classification, second ed., 2001.
[28] C. Köse, U. Şevik, O. Gençalioğlu, Automatic segmentation of age-related macular degeneration in retinal fundus images, Comput. Biol. Med. 38 (5) (2008) 611–619.
[29] C. Köse, U. Şevik, O. Gençalioğlu, C. Ikibaş, T. Kayıkıçıoğlu, A statistical segmentation method for measuring age-related macular degeneration in retinal fundus images, J. Med. Syst. 34 (1) (2010) 1–13.
[30] U.R. Acharya, et al., Automated screening tool for dry and wet age-related macular degeneration (armd) using pyramid of histogram of oriented gradients (phog) and nonlinear features, J. Comput. Sci. 20 (2017).
[31] F.L. Ferris, et al., Clinical classification of age-related macular degeneration, Ophthalmology 120 (4) (2013) 844–851.
[32] C. Agurto, et al., Automatic detection of diabetic retinopathy and age-related macular degeneration in digital fundus images, Invest. Ophthalmol. Vis. Sci. 52 (8) (2011) 5862–5871.
[33] Y. Zheng, M.H.A. Hijazi, F. Coenen, Automated 'disease/ no disease' grading of age-related macular degeneration by an image mining approach, Invest. Ophthalmol. Vis. Sci. 53 (13) (2012).
[34] M.H.A. Hijazi, F. Coenen, Y. Zheng, Data mining techniques for the screening of age-related macular degeneration, Knowl.-Based Syst. 29 (2012) 83–92.
[35] M.H.A. Hijazi, F. Coenen, Y. Zheng, Data mining for amd screening: a classification based approach, Int. J. Simul. Syst. Sci. Technol. 15 (2) (2014) 57–69.
[36] M.R.K. Mookiah, et al., Automated diagnosis of age-related macular degeneration using greyscale features from digital fundus images, Comput. Biol. Med. 53 (2014) 55–64.
[37] M. M.R.K., et al., Decision support system for age-related macular degeneration using discrete wavelet transform, Med. Biol. Eng. Comput. 52 (9) (2014) 781–796.
[38] M.R.K. Mookiah, et al., Automated detection of age-related macular degeneration using empirical mode decomposition, Knowledge-Based Syst. 89 (2015).
[39] M.R.K. Mookiah, et al., Local configuration pattern features for age-related macular degeneration characterization and classification, Comput. Biol. Med. 63 (2015) 208–218.
[40] U.R. Acharya, et al., Novel risk index for the identification of age-related macular degeneration using radon transform and dwt features, Comput. Biol. Med. 73 (2016).
[41] L. Yann, B. Yoshua, G. Hinton, Deep learning, Nature 521 (2015) 436–444.
[42] M. Adhi, J.S. Duker, Optical coherence tomography-current and future applications, Curr. Opin. Ophthalmol. 24 (3) (2013) 213–221.

Jen Hong Tan, Ph.D. is a researcher working in Ngee Ann Polytechnic, Singapore. He completed his B.Eng. (mechanical) and Ph.D. in Nanyang Technological University of Singapore. In the past 10 years, he has published nearly 45 journal papers and co-edited a book. His principal interests are interactive segmentation, computer vision, deep learning and infrared thermography. For more details, see http://jenh.co and https://www.researchgate.net/profile/Jen_Hong_Tan.

Sulatha Bhandary is an additional professor in the department of ophthalmology, Kasturba medical college, Manipal, Manipal University. She is a cataract and retina consultant. She did her in-house training in retina at KMC Manipal. She has special interest in retinal imaging and has various research publications in this specialty. She also has various funded projects to her credit like utilizing indigenous fundus camera for diabetic retinopathy/glaucoma screening. She is a peer reviewer in several journals. She is also performing duties as a deputy director of student affairs in Manipal University.

Sobha Sivaprasad is the Professor of Retinal Clinical Studies in the Institute of Ophthalmology, University College London. She is a Consultant Ophthalmologist at Moorfields Eye Hospital specializing in Medical Retina. Her higher research degree was on age related macular degeneration. She obtained her Medical Retina Fellowship from Moorfields Eye Hospital.

Dr. Sivaprasad has active clinical and laboratory research interests in AMD, diabetic retinopathy and retinal vascular disorders. Her research focuses on biomarkers and modeling of retinal morphology in retinal diseases. She oversees several multicentre clinical trials in these areas and has over 175 peer-reviewed publications to her credit. She is the Editor-in Chief of EYE and a peer reviewer of several ophthalmic journals.

Yuki Hagiwara, B.Eng. is a researcher working in Ngee Ann Polytechnic, Singapore. She completed her B.Eng. (Electrical and Electronics) in Nanyang Technological University of Singapore. In the past year, she has published 35 journal papers. Her main academic interests are artificial intelligence, biomedical imaging, and machine learning. Please see https://www.researchgate.net/profile/Yuki_Hagiwara2 for more details.

Dr. Akanksha Bagchi has completed her MBBS from KMC, Manipal and M.S. Ophthalmology from Maharaja Sayajirao University, Vadodara, India. Her interest lies primarily in medical retina and her M.S. thesis was to compare retinal vessel thickness on fundus photographs in ischemic retinas and normal retinas. Currently, she is a clinical fellow at Epsom and St. Helier Hospital, London and a medical retina research fellow at Moorfield's Eye Hospital, London working under the guidance of Prof. Sobha Sivaprasad focusing on understanding choroidal neovascularization.

U. Raghavendra, Ph.D., is working as faculty in the Department of Instrumentation and Control Engineering, Manipal Institute of Technology, Manipal, India. He received his Ph.D. from Manipal Academy of Higher Education, India. He has published several papers in refereed international SCI-IF journals and international conference proceedings. He has a patent to his credit and received invention award from Intellectual Ventures, USA for his inventions in the year 2014. His major academic interests are in 3D Computer Vision, image processing and Medical image analysis. Please visit https://scholar.google.co.in/citations?user=3nzcDREAAAAJ{&}hl=en for more details.

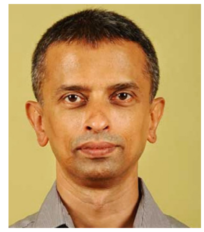

Krishna Rao Addoor is the Professor and Head of the Department of Ophthalmology of Kasturba Medical College Hospital, Manipal, India. He manages various ophthalmic disorders ranging from medical and surgical retinal diseases. He is In-charge of training 250 Undergraduate (MBBS) students and 6 Postgraduate students (MS) per year. He has 19 years of experience in undergraduate and postgraduate training. He is involved in various departmental/ and interdisciplinary research activities, related to Retinal Imaging and Drug delivery system. He is a member of Hospital Infection Control Committee. He has 24 publications to his credit and 152 conference papers & posters in various national and international conferences.

Biju Raju has completed his MBBS from KMC, Manipal and M.S. Ophthalmology from OEU Institute of Ophthalmology, Manipal. He is a Fellow of L.V. Prasad Eye Institute and a Fellow of National Board (FNB) (Vitreoretinal Diseases).

Nitin Shridhara Shetty is currently working as the Head of Department and Head—Retina Services at Department of Ophthalmology, Manipal Hospital, Bangalore.

Arkadiusz Gertych Ph.D., is an Assistant Professor in the Department of Surgery and the Department of Pathology at Cedars-Sinai Medical Center in Los Angeles California. He is also a Research Adjunct Assistant Professor in the Biomedical Engineering Department at the University of Southern California Los Angeles. Dr. Gertych received his Ph.D. degree in Biomedical Electronics at the Silesian University of Technology in Poland. He has published over 100 journal and conference papers, and currently serves as an Associate Editor for Computers in Biology and Medicine. He is also an Editorial Board Member for Informatics in Medicine Unlocked, and has co-edited special issues in Computerized Medical Imaging and Graphics. His scientific interests include bioimage informatics, quantitative image analysis, machine learning and biomedical signal processing.

Chua Kuang Chua is a senior lecturer in Electronic and Computer Engineering Division, Ngee Ann Polytechnic, Singapore. He is the senior manager for Biomedical Engineering Center, Ngee Ann Polytechnic. Kuang Chua received his Ph.D. degree from Queensland University of Technology in 2010. He has published more than 60 journal and conference papers. His major academic interests are in biomedical signal processing, non-linear biosignal processing and artificial intelligent.

U.R. Acharya, Ph.D., Deng is a senior faculty member at Ngee Ann Polytechnic, Singapore. He is also (i) Adjunct Professor at University of Malaya, Malaysia, (ii) Adjunct Faculty at Singapore Institute of Technology—University of Glasgow, Singapore, and (iii) Associate faculty at SIM University, Singapore. He received his Ph.D. from National Institute of Technology Karnataka (Surathkal, India) and Deng from Chiba University (Japan). He has published more than 400 papers, in refereed international SCI-IF journals (345), international conference proceedings (42), books (17) with more than 16,500 citations in Google

Scholar (with h-index of 66), and ResearchGate RG Score of 45.00. **He is ranked in the top 1% of the Highly Cited Researchers (2016, 2017) in Computer Science according to the Essential Science Indicators of Thomson.** He has worked on various funded projects, with grants worth more than 2 million SGD. He has three patents and in the editorial board of many journals. He has served as guest editor for many journals. His major academic interests are in biomedical signal processing, biomedical imaging, data mining, visualization and biophysics for better healthcare design, delivery and therapy. Please visit https://scholar.google.com.sg/citations?user=8FjY99sAAAAJ{&}hl=en for more details.